International Journal of Nanoelectronics and Materials
IJNeaM
ISSN 1985-5761 | E-ISSN 2232-1535

Biodegradable polyhydroxyalkanoate-based microspheres for targeted drug delivery of cefuroxime axetil and propolis

Abdullah Ashraf [a]*, Asra Ali Hussein [a], and Noor S. K. Al-Khafaji [b]

[a] *Department of Polymer and Petrochemical Industries, College of Materials Engineering, University of Babylon, Babylon, Iraq*
[b] *Department of Biology, College of Science, University of Babylon, Babylon, Iraq*
∗Corresponding author. Tel.: +9647710153735; e-mail: abd911370@gmail.com

Received 29 December 2025, Revised 4 March 2026, Accepted 11 March 2026

ABSTRACT

Modern society faces serious environmental issues due to the use of synthetic polymers made from petroleum that do not degrade easily. Other degradable polymers, such as polylactic acid, can cause problems in the human body, including swelling. This has led to a growing focus on creating biodegradable polyhydroxyalkanoates (PHAs). This research aims to use PHAs as a biodegradable microsphere matrix for incorporated medicines such as cefuroxime axetil and propolis, thereby producing drug-loaded microspheres. Using the single-emulsion solvent evaporation technique, PHA microspheres were obtained. FTIR analysis of the extracted PHA, unloaded PHA microspheres (UMs), and drug-loaded microspheres (DLMs) showed no significant chemical changes, confirming the polymer's integrity, with the distinctive PHA peak remaining at 1728.22 cm^{-1}. The SEM test showed successful synthesis of uniform and well-defined spherical particles with an average diameter of approximately 1 μm. The antibacterial activity results showed that cefuroxime axetil had high immediate inhibition, DLMs had lower but effective inhibition, and PHA alone had no antibacterial effect. The zeta potential test of the DLMs yielded a value of -49.5 mV, indicating excellent colloidal stability. The cytotoxicity results for DLMs showed their potential use as targeted anticancer agents against lung cancer cells (A549), with less effect on healthy tissue (human dermal fibroblasts).

Keywords: Polyhydroxyalkanoates, microspheres, drug delivery system, biodegradable polymers

1. INTRODUCTION

Due to the environmental issues caused by the continuous use of synthetic polymers of petroleum origin, the development of biodegradable polymers has attracted the attention of researchers [1]. Biodegradable polymers have been explored as a potential solution to the pollution caused by traditional plastics, such as PHAs [2]. Aliphatic polyesters are made from sustainable feedstocks, while PHAs are directly produced by bacteria through fermentation of a carbon substrate under nutrient-limitation conditions [3]. It is possible to create homo- or copolyesters with various hydroxyalkanoic acids depending on the microorganisms and the cultivation environments [4]. Polyhydroxyalkanoate (PHA) accumulates intracellularly in bacteria as a carbon compound for energy storage [5]. Frequently used bacterial species for PHA production include Bacillus, Pseudomonas, and Cupriavidus, among others [6], [7]. Identification of an effective strain and enhanced PHA production depend on the intended application, which includes formulating the medium and fine-tuning the culture conditions [8]. PHAs are viable substitutes because of their wide range of properties, such as stiffness, brittleness, rubber-like behavior, and resistance to moisture and aroma [9], [10]. These inherent characteristics enable PHAs to be widely used, including in agricultural films and packaging materials [10]. Biodegradable poly(3-hydroxybutyrate) has been used to coat fertilizers that do not contaminate soil and release nitrogen gradually [11]. PHA-based nanofiber membranes have also been investigated for environmental remediation, including water purification, air filtration, and antimicrobial treatments [12]. PHA blends have demonstrated significant potential for use in 3D-printing applications [13]. Furthermore, substances classified as PHAs hold significant promise for medical and pharmaceutical uses [14]. PHAs may also be utilized in the production of dental devices and implant materials. Hydrophobic medications can also be encapsulated by PHA, offering a method for more focused and efficient therapies. In summary, PHA provides environmentally friendly alternatives for medical devices and enhances medication delivery, opening up new avenues in the medical field [15]. Because PHAs decompose into non-toxic products, they are widely used [16]. Biodegradable polymers are employed in medicine for a number of purposes, such as medication delivery systems [17], [18]. Synthetic biodegradable-polymer controlled drug-release microspheres have gained significant attention in the field of drug-delivery systems [19], [20]. Controlled drug release has been a major reason for many studies in the field of microsphere drug-delivery systems (DDS), from which therapeutic agents can be released at regulated rates for extended durations, varying from days to months, thereby offering benefits such as reduced side effects and improved

patient compliance [19], [21]. In 1986, Juni et al. investigated the regulated release of the anticancer antibiotic aclarubicin from poly-β-hydroxybutyric acid (PHB) microspheres. This was among the first studies to investigate the use of PHA microspheres, more specifically those made of PHB, a biodegradable polymer within the PHA family, for controlled pharmaceutical delivery systems [22]. Unlike PLA, which may cause swelling, PHA degrades into non-toxic compounds that do not cause inflammation or swelling in the human body [23], [24]. The non-toxic degradation of PHA made it an excellent candidate for drug-loaded microspheres. Propolis is a resinous substance produced by bees and is regarded as one of the oldest herbal extracts used in medical treatments. Its distinctive attributes are derived from its abundance of flavonoids, phenols, and essential oils, which bestow significant antimicrobial, anti-inflammatory, and antioxidant characteristics, rendering it effective in tissue healing [25], [26]. Furthermore, it has been demonstrated that propolis extract (propolis-EXTR) improves biological processes in stem cells, such as migration, proliferation, and chondrogenic and adipogenic differentiation. Propolis has also been employed as a nanocarrier system because it can successfully lower the virulence of Cryptococcus neoformans in animal models and penetrate an in vitro model of the blood-brain barrier (BBB) [25]. Propolis nanostructured lipid carriers (NLCs) have likewise been used to encourage wound healing and greater skin-regenerative potency [26]. Cefuroxime axetil is a semi-synthetic, broad-spectrum cephalosporin antibiotic used to treat a variety of conditions. It is an oral cephalosporin prodrug that is converted in vivo into its active form, cefuroxime, which is a β-lactam analog [27]. Nonetheless, the use of CA is constrained by biopharmaceutical drawbacks such as inadequate permeability, low solubility, and the need for frequent high concentrations [28], [29]. Nanotechnology-based formulations have been investigated as effective methods to address the drawbacks of uncontrolled biodistribution, unwanted adverse effects, and high-dose administration. Active targeting can also be effectively achieved by conjugating nanomedicines with ligands that specifically target overexpressed receptors. Surface-active targeting ligands on the nanoparticles improve their capacity to target tumor cells (on-target) rather than healthy cells (off-target). As a result, this ligand property reduces related side effects while simultaneously raising the therapeutic index [27]. This study aims to explore PHA's potential for use in the manufacture of microspheres loaded with propolis and cefuroxime axetil for drug-delivery purposes.

2. MATERIALS AND METHODS

The PHA was extracted from a bacterial isolate obtained from a VGO (vacuum gas oil) sample point at Karbala refinery using methods described in previous studies [31], [32]. One hundred milliliters of production medium in a 250 mL Erlenmeyer flask were inoculated with 1% bacterial inoculum, and the flask was then placed in a shaking incubator at 120 rpm and 32°C for 48 hours. The culture was centrifuged for 15 minutes at 5000 rpm, the supernatant was discarded, and the pellet (biomass) was collected and washed with an acetone-ethanol mixture (1:1) and distilled water. Three milliliters of a 10-14% sodium hypochlorite solution were added, followed by 3 mL of chloroform, and the mixture was incubated at 37°C for 2 hours. It was then centrifuged again at 5000 rpm for 20 minutes, producing three layers in the test tube: the lower layer containing PHB dissolved in chloroform, the middle layer containing cellular debris without PHB, and the upper layer containing sodium hypochlorite. The upper layer was discarded using Whatman No. 1 filter paper. The middle and lower layers were filtered, and the lower chloroform layer containing PHB was collected. The chloroform was then evaporated in an oven at 60°C to obtain PHB [31], [32], using glucose as the main carbon source. Propolis was prepared by immersing 15 g of propolis in 75 mL of chloroform solvent, placing it in sealed glass containers, and keeping it in a shaking incubator for the appropriate duration. A Millipore filter (0.22 µm) was then used to filter the solutions. Following extraction, a rotary evaporator was used to concentrate the crude extract, and the samples were kept in a refrigerator at -20 °C until needed [32]. Polyethylene glycol (PEG) 4000 was purchased from HiMedia Laboratories, India.

The single-emulsion solvent-evaporation technique was used to make the microspheres [33], [34], as shown in Figure 1. To make the unloaded PHA microspheres (UMs), two solutions were prepared in separate 50 mL glass beakers using a magnetic stirrer. The first solution contained 0.4 g of PHA and 10 mL of chloroform, while the second contained 0.4 g of PEG and 10 mL of water. No heat was applied. Using a medical syringe, the first solution was added dropwise to the second under high stirring speed. The emulsion mixture was then left on the magnetic stirrer with continuous high stirring until all the chloroform had evaporated, with no heat applied at room temperature. Additional water could be added to cool the mixture or prevent cluster formation. The mixture was centrifuged at 5000 rpm for three minutes after all of the chloroform had evaporated. It was then rinsed with water, centrifuged, and cleaned three or four times. After that, the remaining material was dried for 24 h at 30 °C to remove any moisture. For the drug-loaded microspheres (DLMs), the difference was the addition of a suitable amount of cefuroxime axetil (0.1 g) and propolis (0.1 mL) to the first solution to achieve a 1:4 (w/w) drug-to-polymer ratio.

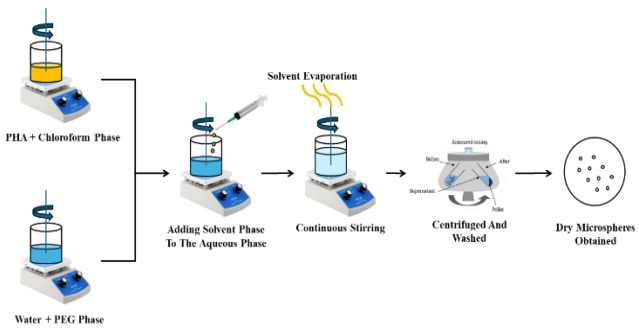

Figure 1. Microspheres synthesis using solvent evaporation technique.

Fourier transform infrared spectroscopy (FTIR) was utilized to analyze the chemical makeup of PHA in three samples: extracted PHA, unloaded PHA microspheres, and drug-loaded PHA microspheres. An inert material, such as 100-200 mg of potassium bromide (KBr), was mixed with 1-2 mg of PHA powder and compressed into a thin pellet. The samples' infrared spectra were recorded between 500 and 4000 cm-1 in wave number. Differential scanning calorimetry (DSC), a thermal analysis method used to examine a material's melting and crystallinity, was employed to analyze how the polymer reacts to temperature changes and to identify important thermal transitions such as the glass transition and melting. Three samples were analyzed using DSC: extracted PHA, unloaded PHA microspheres, and drug-loaded PHA microspheres. A small amount of powder, typically between 5 and 10 mg, was weighed accurately and placed in a DSC aluminum pan, which was then sealed with a lid. The reference was an empty metal pan. Heat flow as a function of temperature was measured using DSC. The samples were heated from 24±1 °C to 250 °C at a scanning rate of 5 °C/min. Scanning electron microscopy (SEM) is an advanced technique used to characterize the morphology and texture of materials at the micrometer level. Its main objective in this regard is to furnish highly detailed images of the sample surface in order to visualize underlying structures and how these structures interact with one another. With the help of a concentrated electron beam, SEM can obtain conclusive data regarding particle form, arrangement, and abnormalities, including voids or pores if present. The sample was dried, placed on a special holder, then inserted into and fixed within the device. Particle charge affects how particles interact with one another and how long they remain dispersed in a liquid medium, regardless of whether the charge is strongly positive or negative. This analysis is particularly crucial in domains such as pharmaceutical delivery systems, where maintaining formulation stability and efficacy requires preventing particle agglomeration, or clumping. In this study, the stability of microspheres in a water dispersant was evaluated using zeta-potential analysis.

2.1. Antibacterial Activity Test

The test was conducted using two bacterial strains, one Gram-positive and one Gram-negative, namely Staphylococcus and Escherichia coli, cultured on two plates of Mueller-Hinton agar, which were incubated at 37°C for 24 h. The bacterial suspension was adjusted to a 0.5 McFarland standard (approximately 1×10^8 CFU/mL). The test was conducted according to Clutterbuck et al. (2007) [32], with some adjustments. Three samples were used for comparison: (1) cefuroxime axetil powder, (2) PHA microspheres loaded with cefuroxime axetil and propolis, and (3) PHA microspheres. Filter paper was cut into 5 mm disk shapes and deposited into 3 mL Eppendorf tubes filled with the samples mentioned above and shaken together. Later, the disks were used in the test and were placed on the cultured Mueller-Hinton agar.

2.2. Cytotoxicity MTT assay

The MTT experiment was used to determine how PHA microspheres loaded with cefuroxime axetil and propolis affected cell survival and cytotoxicity. GraphPad Prism version 10 (GraphPad Software Incorporated, La Jolla, California) was used to determine the IC50, calculate mean±SD values, and draw graphs. Between 5×10^3 and 1×10^4 cells were seeded in each well of a 96-well plate. The cells were then left to adhere for 24 hours at 37 °C with 5% CO_2. The cells were exposed to different concentrations of the drug-loaded PHA microspheres for 24 to 72 hours. Medium alone was added to the control wells to serve as a control. Then 10-20 µL of MTT solution (5 mg/mL in PBS) was added to each well. After that, the plates were incubated for another three to four hours so that mitochondrial dehydrogenases in living cells could convert MTT into purple formazan crystals. After incubation, the supernatant was carefully removed. Then 100-150 µL of dimethyl sulfoxide (DMSO) was added to dissolve the formazan crystals. A microplate reader was used to measure the absorbance at 570 nm, with the background set to 630 nm. To determine the cell-survival rate, the following mathematical equation was used:

$$\text{Cell viability} = \frac{OD\ of\ treated\ cells}{OD\ of\ control\ cells} \times 100\% \qquad (1)$$

In words, cell viability was calculated from the absorbance values of treated, control, and blank wells and then expressed as a percentage. Nonlinear regression analysis was used to determine the half-maximal inhibitory concentration (IC50). After three replicates for each trial, the results were presented as the mean with a standard deviation (SD). The test was based on work done by Maurya et al. (2011) [36].

3. RESULTS AND DISCUSSION

3.1. Fourier Transform Infrared Spectroscopy analysis

The FTIR spectrum of the extracted substance, as shown in Figure 2, clearly demonstrated the hallmarks of PHA, beginning with a pronounced sharp absorption at 1735.93 cm^{-1} that reflects the ester carbonyl (C=O) stretch and serves as an indicator of PHA. Peaks were also observed at 1288.45 cm^{-1} and 1188.15 cm^{-1}, which correspond to C-O and C-O-C stretching vibrations and confirm the presence of ester linkages in the polymer backbone. The spectrum also featured absorptions at 2978.09 cm^{-1} (C-H stretching), 1458.18 cm^{-1} (CH_2 bending), and 1381.03 cm^{-1} (CH_3 bending), all of which underscore the aliphatic nature of the polymer chain. These spectral signatures align closely with previously reported FTIR data for poly(3-hydroxybutyrate) and related PHA copolymers, thereby confirming that the extracted substance is PHA [37], [38].

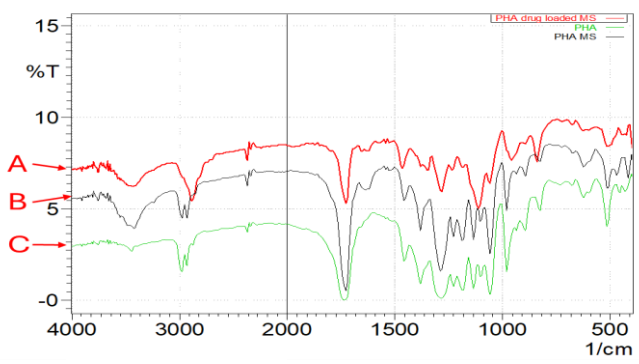

Figure 2. FTIR for (A) drug-loaded PHA microspheres, (B) unloaded PHA microspheres, and (C) extracted PHA.

The FTIR test of the unloaded PHA microspheres showed similarities to the extracted PHA, with only small deviations, as shown by the peaks at 1728.22 cm^{-1} for ester carbonyl (C=O) stretching, 1288.45 cm^{-1} for C-O stretching, 1188.15 cm^{-1} for C-O-C stretching, 2978.09 cm^{-1} for C-H stretching, 1458.18 cm^{-1} for CH_2 bending, and 1381.03 cm^{-1} for CH_3 bending. This indicates that synthesis of the PHA microspheres did not affect the chemical composition or structure of the PHA. These slight deviations may be caused by the physical processing conditions of microsphere formation, such as high-shear mixing and solvent evaporation. There was also a rise in peaks at 3417.86 cm^{-1} and 3464.15 cm^{-1}, which may be due to water residue or PEG residue [39], [40].

For the drug-loaded PHA microspheres, more deviations were observed, some peaks faded away, and new peaks appeared. This suggests that interactions occurred. However, the distinctive PHA peak at 1728 cm^{-1} corresponding to ester carbonyl (C=O) stretching remained, as did the C-O and C-O-C stretching bands at approximately 1288 cm^{-1} and 1188 cm^{-1}, respectively, and the C-H stretching band near 2978 cm^{-1}. In the drug-loaded polymer, the appearance of a new peak at 1111 cm^{-1} may be caused by C-O stretching and C-OH bending between 1362 and 1039 cm-1, resulting from alcohols, ethers, esters, and carboxylic acids representing functional groups in phenolic compounds found in propolis extracts. It may also correspond to C-O-C stretching vibrations characteristic of ether linkages, possibly attributable to the β-lactam ring or sugar moiety present in cefuroxime axetil. The band at 2885 cm^{-1} is likely due to C-H stretching vibrations from aliphatic chains in cefuroxime axetil or to symmetrical and asymmetrical C-H stretching in propolis. There was also broadening at approximately 3425 cm^{-1} and an increase in intensity, which could be due to O-H stretching vibrations arising from hydrogen-bonding interactions between the hydroxyl groups of propolis phenolics [41], [42]. The band at 1465 cm^{-1} can be associated with CH_2 and CH_3 bending vibrations of flavonoid structures in lignin components of propolis [43], [44]. These results demonstrate the successful introduction of cefuroxime axetil and propolis into the PHA microspheres. The new peaks and slight shifts may indicate chemical interactions, such as hydrogen bonding, without significant chemical alterations to the PHA matrix.

3.2. Differential Scanning Calorimetry analysis

The first DSC graph (A in Figure 3) of the extracted PHA shows a melting temperature (Tm) that matches values reported for PHA and polyhydroxybutyrate (PHB), or poly(3-hydroxybutyrate-co-3-hydroxyvalerate) (PHBV), in previous studies [38], [45]. The second graph (B in Figure 3) shows a small new deviation peak at 78 °C, which indicates leftover PEG in the microspheres [46]. Also, there is a decrease in the PHA Tm and heat absorbed, indicating a decrease in crystallinity. In the third DSC graph (C in FIGURE 3), there is a new peak at 233 °C, which may indicate a degradation or some reaction to the added substances. Also, there is a stronger peak at 63 °C, which indicates more leftovers of PEG due to Improper washing or differences in the arrangement of the microsphere's composition [46]. There is also an increase in Tm and heat absorbed this again indicates an increase in crystallinity. The experiment proves that loading the drug into the microspheres does not significantly change the thermal properties of the polymer, only a decrease in crystallinity.

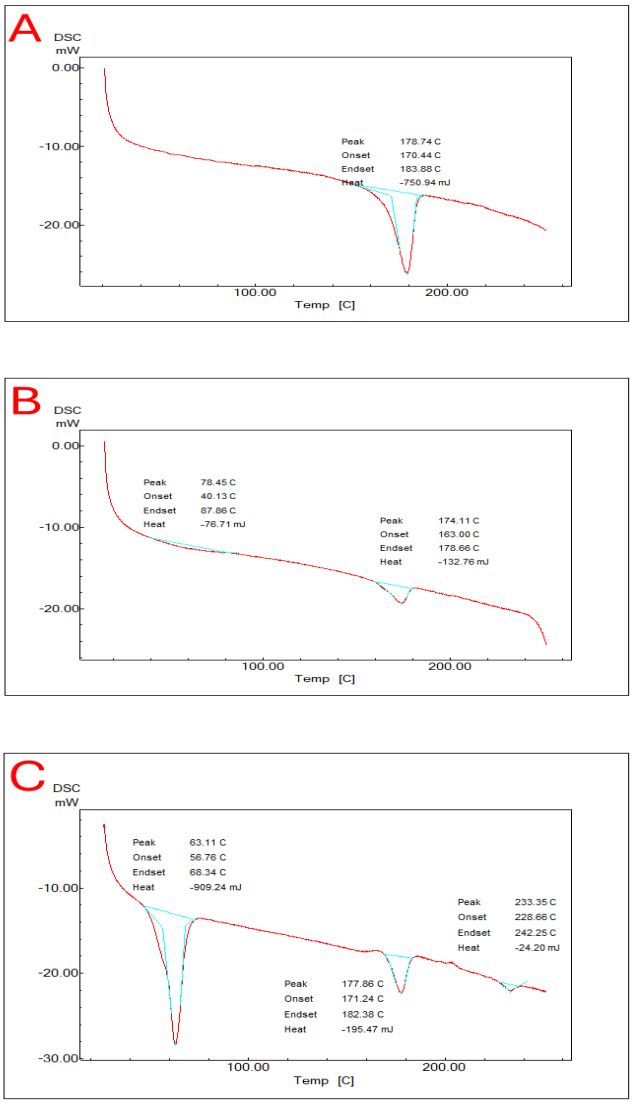

Figure 3. DSC for (A) extracted PHA (B) unloaded PHA microsphere (C) drug-loaded PHA microspheres.

3.3. Scanning Electron Microscope (SEM)

The SEM images prove the successful fabrication of PHAs microspheres with an average diameter of approximately 1 µm. The microspheres have relatively uniform and well-defined spherical shapes. However, the distribution of the microspheres is not entirely homogeneous, and noticeable agglomeration is observed. So, the current method requires some modifications to improve particle dispersion. To minimize microsphere clustering, further optimization of the solvent evaporation method or the utilization of alternative evaporation techniques and equipment may be necessary. To examine the surface morphology and structural properties of the microspheres, a more detailed SEM analysis with higher magnification is required.

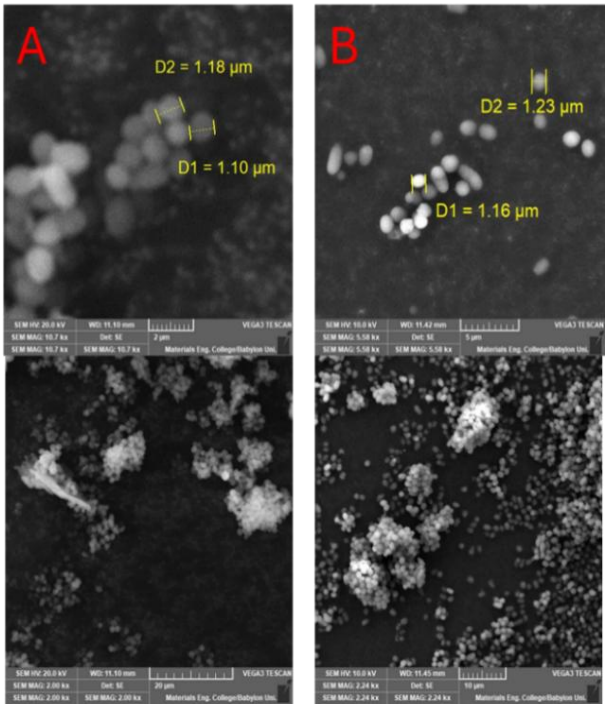

Figure 4. (A) loaded PHA microspheres under SEM (B) PHA microspheres under SEM.

3.4. Antibacterial Activity Test

The test diameter results were sample 1=20 mm, sample 2=12 mm, and sample 3=0 mm for the *Staphylococcus aureus* strain, while for the *Escherichia coli*, it was sample 1=15 mm, sample 2=10 mm, and sample 3=0 mm, as shown in Figure 5. This proves Cefuroxime Axetil has an Instant higher inhibition zone, while the loaded PHA microspheres had a lower inhibition zone, but it was still effective because it had Cefuroxime Axetil and Propolis in its structure. For PHA microspheres, there was no inhibition zone, which means that the PHA has no Antibacterial effect alone. Additional tests are needed to calculate drug release rates. Also, trying different combinations and different concentrations of the added substances is needed to enhance the effectiveness of the microspheres.

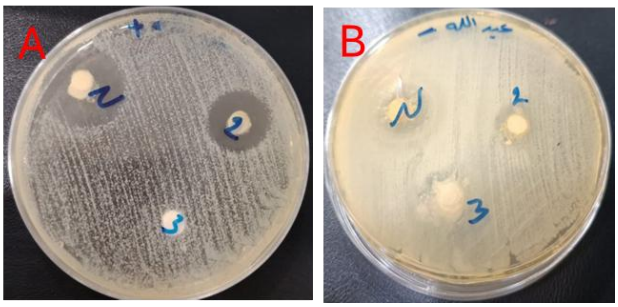

Figure 5. Mueller Hinton Agar (A) *Staphylococcus aureus* (B) *Escherichia coli.*

3.5. Cytotoxicity MTT assay

The treatment's cytotoxicity against human dermal fibroblasts (HDFN) and lung cancer cells (A549) is shown by MTT tests. At 400 µg/mL, the mean and standard deviation of HDFN cells were much higher than those of A549 cells, at 72.02 ±0.87 and 38.42 ± 1.10 (mean and SD, respectively). The fact that HDFN cells lived longer at 400 µg/mL shows that the treatment is less harmful or incompatible with normal fibroblasts, as shown by the higher mean and lower SD. (Table 1)

Table 1. Comparison of mean and SD cell inhibition of A549 with HDFN treated with drug-loaded PHA microspheres (25,50,100,200, 400،µg/mL)for 24h.

1	HDFN		A549	
Conc.	mean	SD	mean	SD
400	72.02	0.87	38.42	1.10
200	76.81	1.21	49.57	1.75
100	88.07	0.94	61.535	1.06
50	93.48	0.40	74.15	2.08
25	95.48	0.23	87.03	1.85

Table 1 illustrates how the polymer attacks cancer cells while simultaneously safeguarding healthy ones. When the quantity is 400 µg/mL, A549 cells become less active, which suggests that there is more cell death for cancer cells. As a result, this treatment has a lot of potential for treating cancer. This harmful effect could be caused by a number of things. The molecules that make up cancer cells, like A549, are very different from those that make up normal cells. This makes it harder for cancer cells to take in and use substances. Baskar et al. say that A549 cells may be more vulnerable to harmful chemicals because their death pathways are not working properly. The longer life span at the studied concentration is probably because HDFN cells are not cancerous and may have stronger protection against oxidative stress and other damage to cells caused by treatment. The best treatment dosage is very important because it affects how harmful the treatment is to both normal and cancerous cells. Some substances, whether they are man-made or natural, may be able to target cancer cells only while protecting healthy cells from harm, according to an early study. Zhao and others created

nanoparticles that hold PTX using a biodegradable material known as Poly(glycolide-co-ε-caprolactone)-b-D-α-tocopheryl polyethylene glycol 2000 succinate, which are smooth and 200 nanometers in size[47]. These were smooth-surfaced 200-nm nanoparticles. They had better drug loading and encapsulation than PLGA nanoparticles. These nanoparticles outperformed Taxol in vitro against A549 lung cancer cells. PTX loaded with nanoparticles showed better results in stopping the tumor than Taxol.

The statistical study showed a significant difference in the viability of HDFN cells compared with A549 cells. This suggests that the therapy could be used to treat cancer. To determine whether the substance could be used for targeted cancer treatment, gene-expression studies or apoptosis tests should be used to investigate the molecular processes underlying selective cytotoxicity.

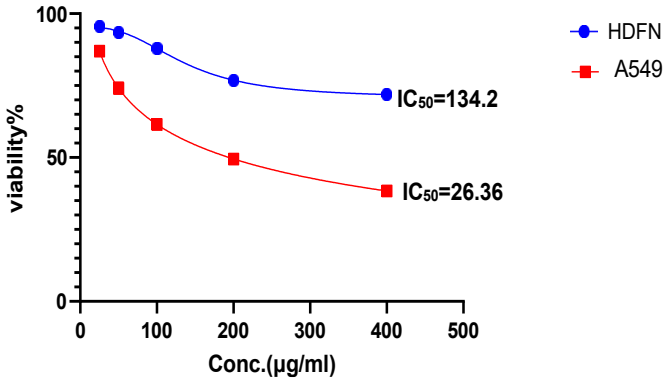

Figure 6. IC50 of HDFN and A549 treated with polymer (polyhydroxy alkinate + polyethylene glycol).

The damaging effects of the polyhydroxyalkanoate + polyethylene glycol (PHA + PEG) mixture are clearly different in HDFN (human dermal fibroblasts) and A549 (human lung cancer) cells, as demonstrated by the IC50 values from the MTT test. HDFN cells showed an IC50 of 134 µg/mL, whereas A549 cells showed an IC50 of only 26 µg/mL. These results indicate that the PHA + PEG mixture is more harmful to cancer cells than to normal fibroblasts, making it a potential option for targeted cancer treatment. The higher IC50 value for HDFN cells indicates that a larger concentration of the PHA + PEG blend is needed to reduce fibroblast viability by 50%, which means it is less harmful to normal cells. The lower IC50 value for A549 cells shows that cancer cells are more sensitive to the treatment and therefore require a much lower concentration to achieve the same level of inhibition. This differential response is an important step toward reducing the harmful side effects of traditional chemotherapy and suggests that PHA + PEG may be useful as a targeted cancer treatment. IC50 values differ between normal and cancerous cells because of differences in their molecular and metabolic behavior. Cancer cells such as A549 are more likely to respond to treatments that interrupt cell function because of their rapid growth, altered apoptosis mechanisms, and increased metabolic activity. Normal cells, including HDFN, have stronger regulatory mechanisms, including better DNA repair and apoptosis pathways, which help protect them from treatment-induced damage (Ahmad et al., 2019) [48]. Based on these results, using PHA + PEG nanoparticles to treat cancer might effectively kill cancer cells while doing little harm to healthy tissues. Future research should focus on testing PHA + PEG in living organisms, understanding its mode of action, and checking for any long-term adverse effects to better assess its possible medical uses [47], [48], [49]. In addition, trying different combinations and concentrations of the incorporated substances is needed to enhance the effectiveness of the microspheres.

3.6. Zeta potential test

Zeta-potential measurements were used to assess the stability of the PHA drug-loaded microspheres; the test revealed how these particles sustained their dispersion and resisted aggregation over time. In general, a stable dispersion is indicated by a zeta potential greater than +30 mV or less than -30 mV, while values closer to zero suggest an increase in agglomeration and instability over time [50], [51]. The zeta-potential test of the drug-loaded PHA microspheres showed a value of -49.5 mV, indicating excellent colloidal stability [52], as shown in Figure 7. This highly negative surface charge suggests strong electrostatic repulsion between the microspheres, which effectively prevents aggregation and supports long-term dispersion in suspension. As shown in previous studies, stable particles are indicated by zeta-potential values of ±30 mV; hence, the measured zeta potential verifies that the created PHA microspheres have the required surface properties to resist agglomeration. These findings point to the effective design of a stable drug-delivery system with desirable physicochemical characteristics for biomedical uses.

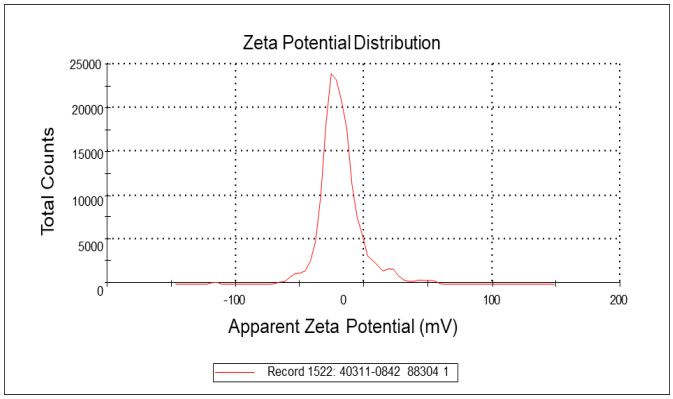

Figure 7. Zeta potential result of PHA drug loaded microspheres.

4. CONCLUSION

In this study, the produced PHA was characterized and used to synthesize PHA-loaded microspheres. FTIR and DSC analyses of the extracted substances showed patterns matching PHA and PHB in previous studies. FTIR and DSC also showed that the synthesis of PHA microspheres and the incorporation of cefuroxime axetil and propolis did not affect the chemical composition or structure of the PHA.

The SEM test confirmed the successful synthesis of symmetric spherical microspheres with an average diameter of approximately 1 μm. Antibacterial activity demonstrated the success and effectiveness of adding cefuroxime axetil and propolis by giving PHA antibacterial properties that it did not have before their addition. The MTT assay also showed differential cytotoxicity of the PHA microspheres loaded with cefuroxime axetil and propolis against human lung cancer cells (A549) compared with normal human dermal fibroblasts (HDFN). At a concentration of 400 μg/mL, the microspheres reduced A549 cell survivability to 38.4%, while HDFN cells maintained 72.0% survivability, indicating that the drug-loaded PHA microspheres effectively inhibit cancer-cell proliferation with minimal harm to healthy tissues. The zeta-potential test of the drug-loaded PHA microspheres showed a value of -49.5 mV, indicating excellent colloidal stability and suggesting that the microspheres will not readily agglomerate in the bloodstream. While the synthesis of drug-loaded microspheres was successful, more testing is still needed to measure drug-loading efficiency, drug-release rates, and in vivo performance to assess tumor regression and systemic toxicity.

REFERENCES

[1] A. R. Yasin and I. K. Al-Mayaly, “Isolation and identification of polyhydroxyalkanoates producing bacteria from biopolymers waste in soil,” IOP Conf Ser Mater Sci Eng, vol. 928, no. 6, Nov. 2020, doi: 10.1088/1757-899X/928/6/062014.

[2] A. Samir, F. H. Ashour, A. A. A. Hakim et al., "Recent advances in biodegradable polymers for sustainable applications," npj Mater. Degrad., vol. 6, art. no. 68, 2022, doi: 10.1038/s41529-022-00277-7.

[3] A. A. Hussein, N. Kaddim Radi, and N. Mohammed Sahi, "Integrative computational and experimental study of propolis, polyvinyl alcohol, and Alhagi maurorum complex as anticancer and antibacterial agents," J. Biomater. Sci. Polym. Ed., vol. 36, no. 12, pp. 1718–1748, Aug. 2025, doi: 10.1080/09205063.2025.2464448.

[4] F. Muneer, I. Rasul, F. Azeem, M. H. Siddique, M. Zubair, and H. Nadeem, “Microbial Polyhydroxyalkanoates (PHAs): Efficient Replacement of Synthetic Polymers,” Journal of Polymers and the Environment 2020 28:9, vol. 28, no. 9, pp. 2301–2323, Jun. 2020, doi: 10.1007/S10924-020-01772-1.

[5] A. B. Akinmulewo and O. C. Nwinyi, “Polyhydroxyalkanoate: a biodegradable polymer (a mini review)”, doi: 10.1088/1742-6596/1378/4/042007.

[6] M. S. Morlino et al., “Cupriavidus necator as a platform for polyhydroxyalkanoate production: An overview of strains, metabolism, and modeling approaches,” Biotechnol Adv, vol. 69, p. 108264, Dec. 2023, doi: 10.1016/J.BIOTECHADV.2023.108264.

[7] N. Iftikhar, I. Ali, F. Quddus, M. U. Raza, N. Nadeem, and M. Zaid, “Production of Polyhydroxyalkanoates (pha) by bacillus and pseudomonas on Cheap Carbon Substrates,” Brazilian Archives of Biology and Technology, vol. 67, p. e24230082, Jul. 2024, doi: 10.1590/1678-4324-2024230082.

[8] M. Li and M. R. Wilkins, “Recent advances in polyhydroxyalkanoate production: Feedstocks, strains and process developments,” Int J Biol Macromol, vol. 156, pp. 691–703, Aug. 2020, doi: 10.1016/J.IJBIOMAC.2020.04.082.

[9] S. A. Acharjee, P. Bharali, B. Gogoi, V. Sorhie, B. Walling, and Alemtoshi, “PHA-Based Bioplastic: a Potential Alternative to Address Microplastic Pollution,” Water Air Soil Pollut, vol. 234, no. 1, p. 21, Jan. 2022, doi: 10.1007/S11270-022-06029-2.

[10] A. Z. Naser, I. Deiab, F. Defersha, and S. Yang, "Expanding poly(lactic acid) (PLA) and polyhydroxyalkanoates (PHAs) applications: A review on modifications and effects," Polymers, vol. 13, no. 23, art. no. 4271, Dec. 2021, doi: 10.3390/polym13234271.

[11] S. Kontárová et al., "Slow-release nitrogen fertilizers with biodegradable poly(3-hydroxybutyrate) coating: Their effect on the growth of maize and the dynamics of N release in soil," Polymers, vol. 14, no. 20, art. no. 4323, Oct. 2022, doi: 10.3390/polym14204323.

[12] S. A. Al-Mutwalli, M. N. Taher, B. Ciftcioglu-Gozuacik, D. Y. Koseoglu-Imer, and F. Lipnizki, "Polyhydroxyalkanoate (PHA)-based electrospun nanofibers in environmental applications: Advances, limitations, and prospects," J. Environ. Chem. Eng., vol. 13, no. 6, art. no. 120431, Dec. 2025, doi: 10.1016/j.jece.2025.120431.

[13] M. Ďurfina et al., "Bio-based polyhydroxyalkanoate (PHA) blends for 3D printing: Rheological, mechanical, biocompatibility, and biodegradation properties," Polymers, vol. 17, no. 11, art. no. 1477, May 2025, doi: 10.3390/polym17111477.

[14] F. Kurul, H. Turkmen, A. E. Cetin, and S. N. Topkaya, "Nanomedicine: How nanomaterials are transforming drug delivery, bio-imaging, and diagnosis," Next Nanotechnology, 2024, doi: 10.1016/j.nxnano.2024.100129.

[15] R. Ben Abdeladhim, J. A. Reis, A. M. Vieira, and C. D. de Almeida, "Polyhydroxyalkanoates: Medical applications and potential for use in dentistry," Materials, vol. 17, no. 22, art. no. 5415, Nov. 2024. [Online]. Available: https://doi.org/10.3390/ma17225415,

[16] A. R. Yasin and I. K. Al-Mayaly, “Study of the Fermentation Conditions of the Bacillus Cereus Strain ARY73 to Produce Polyhydroxyalkanoate (PHA) from Glucose,” Journal of Ecological Engineering, vol. 22, no. 8, pp. 41–53, 2021, doi: 10.12911/22998993/140326.

[17] X. Zhang et al., “A Polyhydroxyalkanoates-Based Carrier Platform of Bioactive Substances for Therapeutic Applications,” Front Bioeng Biotechnol,

vol. 9, p. 798724, Jan. 2022, doi: 10.3389/FBIOE.2021.798724/PDF.

[18] A. Shrivastav, H. Y. Kim, and Y. R. Kim, "Advances in the Applications of Polyhydroxyalkanoate Nanoparticles for Novel Drug Delivery System," Biomed Res Int, vol. 2013, p. 581684, 2013, doi: 10.1155/2013/581684.

[19] Y. J. Lee and M. S. Kim, "Advances in drug-loaded microspheres for targeted, controlled, and sustained drug delivery: Potential, applications, and future directions," Biomed. Pharmacother., vol. 189, art. no. 118244, 2025, doi: 10.1016/j.biopha.2025.118244.

[20] M. Winnacker and B. Rieger, "Copolymers of polyhydroxyalkanoates and polyethylene glycols: recent advancements with biological and medical significance," Polym Int, vol. 66, no. 4, pp. 497–503, Apr. 2017, doi: 10.1002/PI.5261.

[21] T. C. Ezike et al., "Advances in drug delivery systems, challenges and future directions," Heliyon, vol. 9, no. 6, art. no. e17488, Jun. 2023, doi: 10.1016/j.heliyon.2023.e17488.

[22] J. Kazuhiko, N. Masahiro, and K. Miho, "Controlled release of aclarubicim, an anticancer antibiotic, from poly-β-hydroxybutyric acid microspheres," Journal of Controlled Release, vol. 4, no. 1, pp. 25–32, Jun. 1986, doi: 10.1016/0168-3659(86)90030-1.

[23] C. S. Proikakis, N. J. Mamouzelos, P. A. Tarantili, and A. G. Andreopoulos, "Swelling and hydrolytic degradation of poly(d,l-lactic acid) in aqueous solutions," Polym Degrad Stab, vol. 91, no. 3, pp. 614–619, Mar. 2006, doi: 10.1016/J.POLYMDEGRADSTAB.2005.01.060.

[24] P. Chaber et al., "Enhancing the Potential of PHAs in Tissue Engineering Applications: A Review of Chemical Modification Methods," Materials 2024, Vol. 17, Page 5829, vol. 17, no. 23, p. 5829, Nov. 2024, doi: 10.3390/MA17235829.

[25] P. Thammasit et al., "Targeted Propolis-Loaded Poly (Butyl) Cyanoacrylate Nanoparticles: An Alternative Drug Delivery Tool for the Treatment of Cryptococcal Meningitis," Front Pharmacol, vol. 12, p. 723727, Aug. 2021, doi: 10.3389/FPHAR.2021.723727/BIBTEX.

[26] O. M. Elkhateeb, M. E. I. Badawy, A. E. Noreldin, H. M. Abou-Ahmed, M. H. El-Kammar, and H. A. Elkhenany, "Comparative evaluation of propolis nanostructured lipid carriers and its crude extract for antioxidants, antimicrobial activity, and skin regeneration potential," BMC Complement Med Ther, vol. 22, no. 1, pp. 1–13, Dec. 2022, doi: 10.1186/S12906-022-03737-4/FIGURES/7.

[27] A. Yadav, N. Yadav, R. Rawat, S. Sharma, T. Gupta, and D. Prasad, "Advancing Cefuroxime Axetil through Nanotechnology: Enhancing Its Effectiveness," J BioX Res, vol. 7, Dec. 2024, doi: 10.34133/JBIOXRESEARCH.0023/ASSET/ECCC342A-3049-4EEC-88D7-E56FF48F8139/ASSETS/GRAPHIC/JBIOXRESEARCH.0023.FIG.002.JPG.

[28] M. Monzón et al., "A simple infection model using pre-colonized implants to reproduce rat chronic Staphylococcus aureus osteomyelitis and study antibiotic treatment," Journal of Orthopaedic Research, vol. 19, no. 5, pp. 820–826, Sep. 2001, doi: 10.1016/S0736-0266(00)00076-0.

[29] B. Singh, P. R. Vuddanda, V. M.R., V. Kumar, P. S. Saxena, and S. Singh, "Cefuroxime axetil loaded solid lipid nanoparticles for enhanced activity against S. aureus biofilm," Colloids Surf B Biointerfaces, vol. 121, pp. 92–98, Sep. 2014, doi: 10.1016/J.COLSURFB.2014.03.046.

[30] A. Soam, A. K. Singh, R. Singh, and S. K. Shahi, "Optimization of culture conditions for bio-polymer producing Bacillus mycoides (WSS2) bacteria from sewage," Current Discovery, vol. 1, no. 1, pp. 27–32, 2012.

[31] S. K. Hahn, Y. K. Chang, B. S. Kim, and H. N. Chang, "Optimization of microbial poly(3-hydroxybutyrate) recover using dispersions of sodium hypochlorite solution and chloroform," Biotechnol Bioeng, vol. 44, no. 2, pp. 256–261, 1994, doi: 10.1002/BIT.260440215.

[32] L. Kubiliene et al., "Alternative preparation of propolis extracts: Comparison of their composition and biological activities," BMC Complement Altern Med, vol. 15, no. 1, pp. 1–7, Dec. 2015, doi: 10.1186/S12906-015-0677-5/TABLES/3.

[33] Y. Huang, A. Stonehouse, and C. Abeykoon, "Encapsulation methods for phase change materials – A critical review," Int J Heat Mass Transf, vol. 200, p. 123458, Jan. 2023, doi: 10.1016/j.ijheatmasstransfer.2022.123458.

[34] A. Anjum, M. Zuber, K. M. Zia, A. Noreen, M. N. Anjum, and S. Tabasum, "Microbial production of polyhydroxyalkanoates (PHAs) and its copolymers: A review of recent advancements," Int J Biol Macromol, vol. 89, pp. 161–174, Aug. 2016, doi: 10.1016/J.IJBIOMAC.2016.04.069.

[35] A. L. Clutterbuck, C. A. Cochrane, J. Dolman, and S. L. Percival, "Evaluating antibiotics for use in medicine using a poloxamer biofilm model," Ann Clin Microbiol Antimicrob, vol. 6, 2007, doi: 10.1186/1476-0711-6-2.

[36] D. K. Maurya, N. Nandakumar, and T. P. A. Devasagayam, "Anticancer property of gallic acid in A549, a human lung adenocarcinoma cell line, and possible mechanisms," J Clin Biochem Nutr, vol. 48, no. 1, pp. 85–90, Jan. 2010, doi: 10.3164/jcbn.11-004FR.

[37] A. V. Samrot et al., "The Synthesis, Characterization and Applications of Polyhydroxyalkanoates (PHAs) and PHA-Based Nanoparticles," Polymers (Basel), vol. 13, no. 19, p. 3302, Oct. 2021, doi: 10.3390/POLYM13193302.

[38] A. R. Yasin and I. k. Al-Mayaly, "Biosynthesis of polyhydroxyalkanoate (PHA) by a newly isolated strain Bacillus tequilensis ARY86 using inexpensive carbon source," Bioresour Technol Rep, vol. 16, p. 100846, Dec. 2021, doi: 10.1016/J.BITEB.2021.100846.

[39] F. Dai, Q. Zhuang, G. Huang, H. Deng, and X. Zhang, "Infrared Spectrum Characteristics and

Quantification of OH Groups in Coal," ACS Omega, vol. 8, no. 19, pp. 17064–17076, May 2023, doi: 10.1021/ACSOMEGA.3C01336/ASSET/IMAGES/LARGE/AO3C01336_0011.JPEG.

[40] S. W. Jun et al., "Cefuroxime axetil solid dispersions prepared using solution enhanced dispersion by supercritical fluids," J Pharm Pharmacol, vol. 57, no. 12, pp. 1529–1537, Dec. 2005, doi: 10.1211/JPP.57.12.0003.

[41] C. da Silva, A. Prasniewski, M. A. Calegari, V. A. de Lima, and T. L. C. Oldoni, "Determination of Total Phenolic Compounds and Antioxidant Activity of Ethanolic Extracts of Propolis Using ATR–FT-IR Spectroscopy and Chemometrics," Food Anal Methods, vol. 11, no. 7, pp. 2013–2021, Jul. 2018, doi: 10.1007/S12161-018-1161-X/METRICS.

[42] U. Erdogan, "Ultrasonic assisted propolis extraction: characterization by ATR-FTIR and determination of its total antioxidant capacity and radical scavenging ability," International Journal of Secondary Metabolite, vol. 10, no. 2, pp. 231–239, Jun. 2023, doi: 10.21448/IJSM.1167773.

[43] C. Akcay, E. Birinci, C. Birinci, and S. Kolayli, "Durability of wood treated with propolis," Bioresources, vol. 15, no. 1, pp. 1547–1562, Feb. 2020, doi: 10.15376/BIORES.15.1.1547-1562.

[44] A. G. Hegazi, A. S. El-Houssiny, and E. A. Fouad, "Egyptian propolis 14: Potential antibacterial activity of propolis-encapsulated alginate nanoparticles against different pathogenic bacteria strains," Advances in Natural Sciences: Nanoscience and Nanotechnology, vol. 10, no. 4, p. 045019, Nov. 2019, doi: 10.1088/2043-6254/AB52F4.

[45] S. Hlaváčiková et al., "The possibility of using the regranulate of a biodegradable polymer blend based on polylactic acid and polyhydroxybutyrate in FDM 3D printing technology," Results in Materials, vol. 21, p. 100511, Mar. 2024, doi: 10.1016/J.RINMA.2023.100511.

[46] P. Johansson et al., "Cycling stability of poly(ethylene glycol) of six molecular weights: Influence of thermal conditions for energy applications," ACS Appl Energy Mater, vol. 3, no. 11, pp. 10578–10589, Nov. 2020, doi: 10.1021/ACSAEM.0C01621/ASSET/IMAGES/MEDIUM/AE0C01621_M005.GIF.

[47] T. Zhao et al., "Paclitaxel-loaded poly(glycolide-co-ε-caprolactone)-b-D-α-tocopheryl polyethylene glycol 2000 succinate nanoparticles for lung cancer therapy," Int J Nanomedicine, vol. 8, pp. 1947–1957, 2013, doi: 10.2147/IJN.S44220.

[48] A. Ahmad, F. Khan, R. K. Mishra, and R. Khan, "Precision Cancer Nanotherapy: Evolving Role of Multifunctional Nanoparticles for Cancer Active Targeting," J Med Chem, vol. 62, no. 23, pp. 10475–10496, Dec. 2019, doi: 10.1021/ACS.JMEDCHEM.9B00511.

[49] A. A. Hussein, N. Kaddim Radi, and N. Mohammed Sahi, "Integrative computational and experimental study of propolis, polyvinyl alcohol, and alhagi maurorum complex as anticancer and antibacterial agents," J Biomater Sci Polym Ed, 2025, doi: 10.1080/09205063.2025.2464448.

[50] R. A. Kepekçi, B. Yener İlçe, and S. Demir Kanmazalp, "Plant-derived biomaterials for wound healing," Studies in Natural Products Chemistry, vol. 70, pp. 227–264, Jan. 2021, doi: 10.1016/B978-0-12-819489-8.00001-6.

[51] H. Valizadeh, A. Farajnia, and P. Zakeri-Milani, "Formulation of cefuroxime axetil oral suspension and investigation of its pharmaceutical properties," Adv Pharm Bull, vol. 1, no. 2, pp. 93–96, 2011, doi: 10.5681/APB.2011.014,.

[52] F. A. El-malek, M. Rofeal, A. Farag, S. Omar, and H. Khairy, "Polyhydroxyalkanoate nanoparticles produced by marine bacteria cultivated on cost effective Mediterranean algal hydrolysate media," J Biotechnol, vol. 328, pp. 95–105, Feb. 2021, doi: 10.1016/J.JBIOTEC.2021.01.008.